EVALUATION OF A UAV-BASED HYPERSPECTRAL FRAME CAMERA FOR MONITORING THE LEAF NITROGEN CONCENTRATION IN RICE

*Hengbiao Zheng, Xiang Zhou, Tao Cheng, Xia Yao, Yongchao Tian, Weixing. Cao, Yan Zhu**

National Engineering and Technology Center for Information Agriculture (NETCIA),
Jiangsu Key Laboratory for Information Agriculture,
Jiangsu Collaborative Innovation Center for Modern Crop Production,
Nanjing Agricultural University, Nanjing, Jiangsu, China
2015201019@njau.edu.cn, yanzhu@njau.edu.cn

ABSTRACT

UAV based hyperspectral imaging is a promising approach to monitor crop growth status rapidly and non-destructively. This paper described a novel instrument to get hyperspectral information from lightweight unmanned aerial vehicles for crop monitoring. The objectives of this study were to assess the data quality of one hyperspectral frame camera and evaluate the ability in rice nitrogen status monitoring. In this study, we introduced one hyperspectral frame camera weighing 470g which could be mounted to low-weight UAVs (<3 kg). The flight campaign was conducted in a paddy rice field in September 2015. During the flight, two ground-based portable spectrometers (ASD Field Spec Pro spectrometer and GreenSeeker RT 100) were used to collect rice canopy spectra. Later, Normalized difference vegetation index (NDVI) derived from hyperspectral images was compared with that from GreenSeeker and ASD. Also, field sampling was taken at the same day with the flight, and leaf nitrogen concentration (LNC) was obtained through Kjeldahl digestion method. Five existing vegetation indices that were used for N detection were used to estimate LNC. Results are satisfactory, which lay a foundation for the promising application of UAV-based hyperspectral remote sensing on precision agriculture.

Index Terms- UAV, hyperspectral camera, hyperspectra, GreenSeeker, leaf nitrogen concentration, vegetation index, rice

1. INTRODUCTION

Nitrogen (N) is one of the indispensable elements for rice growth, and the management of N fertilization is the goal of intense research efforts in the world [1-2]. To date, nitrogen fertilizer is often applied in excess of crop needs, resulting in economic loss and environmental pollution [3]. Therefore, efficient N management is emergent in modern agriculture.

Hyperspectral remote sensing has been successfully applied to the detection of crop monitoring with field spectrometers, airborne sensors or satellites [4-6]. Recently, ultra-light weight spectrometers have been introduced into the market, which makes light weight UAV-based hyperspectral imaging come true.

The aim of this study is to evaluate a new instrument one lately available hyperspectral frame camera, the Cubert UHD185, and test its ability in rice nitrogen status monitoring. The system weighs less than 1 kg and is able to produce hyperspectral images. While the reliability of spectra from this instrument has not been reported in public, and few work has been done about the application of this camera in rice nitrogen monitoring.

2. STUDY AREA AND DATA ACQUISITION

2.1. Study site

The study site is located in Rugao city, Jiangsu province, China (120°19'E, 32°14'N). Two cultivars (WYJ and YLY) were seeded on 15 May and transplanted on 16 June, and the plot size was 6 m by 5 m. A randomized complete block design was set up with 4 N fertilizer rates (total N input): 0, 100, 200 and 300 kg N ha^{-1} as urea, corresponding with N0, N1, N2 and N3, respectively. For all treatments, 135 kg/ha P_2O_5 (as monocalcium phosphate [$Ca(H_2PO_4)_2$]) and 200 kg/ha K_2O (as KCl) were applied prior to transplanting. Other management procedures were according to the local standard practices for rice production.

2.2. Ground-based spectra measurements

Rice canopy spectral reflectance were collected by two sensors: (1) ASD Field Spec Pro spectrometer (Analytical Spectral Devices, Boulder, CO, USA), abbreviated as ASD; (2) GreenSeeker RT 100 (NTech Industries, Ukiah, CA, USA), abbreviated as GS.

For ASD spectra measurements, three scan positions within one plot representing a typical crop cover were randomly taken (Fig. 1). The three measurements were averaged to represent a mean plot spectrum and resampled based on the Cubert's spectral sampling. While, GS was run crosswise according to the row direction, and 3 rows of each plot were measured (Fig. 1). In addition, the data obtained from GS was NDVI. All reflectance spectra measurements

Table 1
Summary of spectral indices studied in this paper.

Index	Formula	References
VIopt	$(1+0.45)((R_{800})^2+1)/(R_{670}+0.45)$	[7]
MCARI/MTVI2	MCARI/MTVI2 $MCARI=(R_{700}-R_{670}-0.2(R_{700}-R_{550}))(R_{700}/R_{670})$ $MTVI2=1.5(1.2(R_{800}-R_{550})-2.5(R_{670}-R_{550}))/sqrt((2R_{800}+1)^2-(6R_{800}-5sqrt(R_{670}))-0.5)$	[8]
R-M	$R_{750}/R_{720}-1$	[9]
REP	$700+40((R_{670}+R_{780})/2-R_{700})/(R_{740}-R_{700})$	[10]
NDVI	$(R_{800}-R_{670})/(R_{800}+R_{670})$	[11]

Ri denotes reflectance at band i (nanometer); As the spectral sampling of the camera is 4nm, bands in the formula are chosen the closest bands.

were taken from 11 am to 2 pm local mean time around solar noon, under mostly cloudless conditions.

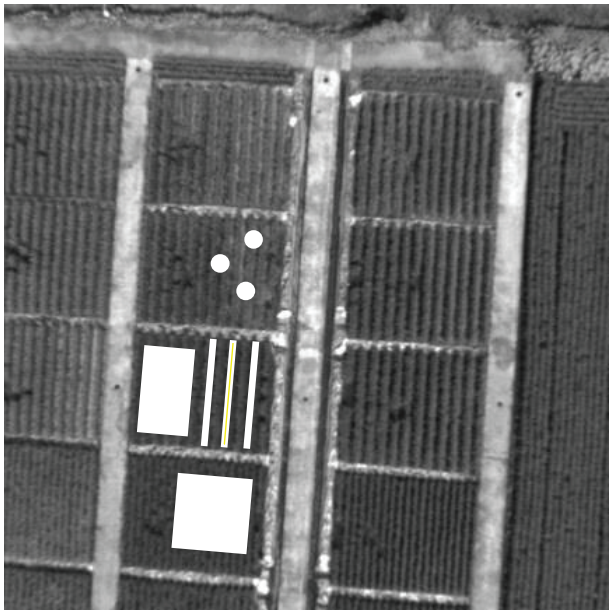

Fig. 1. Circles were three hyperspectral measurements captured with the FieldSpec4; Square was digitized for calculating spatial statistics of the hyperspectral images; Rectangle was the plant sampling region; Strips were three active spectrometer measurements captured with GreenSeeker; plot size is 5 m by 6 m.

2.3. UAV campaign

UAV campaign was conducted in the rice field on September 3rd. As UAV platform, a HiSystems's MK OktoXL (www.mikrokopter.de) was used. The Mk OktoXL is a low-cost and low-weight UAV. Take-off weight without sensors is 1.83 kg. Payloads of up to 2.5 kg are possible and result in a flight time of about 15 minutes depending on the battery. The hyperspectral camera used in the campaign is the Cubert UHD 185. It is a hyperspectral frame camera which provides 138 channels in a spectral range of 450 nm to 950 nm with a spectral sampling of 4 nm. The camera weights 470 g and is calibrated against a white panel.

The camera was flown at 50 m above canopy and the spatial resolution of the camera was about 34 cm. A polygon was selected for each plot excluding bordering effects to produce with spatial statistics a mean spectrum from the hyperspectral images (Fig. 1).

2.4. Determination of rice leaf nitrogen concentration

After the flight, plants for growth analysis were sampled from three hills in each plot. All green leaves were separated from stems and oven-dried at 80°C and weighed. Dried leaf samples were ground and passed through a 1-mm sieve, and stored in plastic bags for further analysis. LNC was determined by using the micro-Keldjahl method.

2.5. Spectral indices for comparison

Five spectral indices considered to be good candidates for estimating plant N concentration were tested. Included were indices specifically aimed at N estimation (N concentration) as well as some indices aimed at chlorophyll estimation (chlorophyll concentration) (Table 1).

3. RESULTS AND DISCUSSIONS

3.1. Spectral comparison between ASD and hyperspectral camera

The derived mean spectra from the UAV-campaign with the UHD 185 and the FieldSpec4 field measurements are displayed in Fig. 2. The solid lines in different thickness represent the spectra from the UHD 185 at different N rates while the dashed lines represent the spectra from ASD. The general trend of the mean spectra derived from the different sensors at different N rates are showing a similar trend: as the N rates increases, the reflectance in near infrared region increases, while the reflectance in visible region decreases. Furthermore, an apparent spectral saturation phenomenon appears at high N rate (N2 and N3).

Spectral difference is calculated by ($Ref_{image} - Ref_{ASD}$)/Ref_{image}). Little spectral difference is found in red edge and near infrared region (706 nm-718 nm and 762 nm-886 nm), with a rate of below 5%. In visible region, reflectance values from image are higher than that of ASD. The spectra do not match perfectly, which is not surprising. Because the spatially derived mean spectra include a much higher spectral variation representing soil reflectance and

canopy structure variations, while for the FieldSpec4 spectra more homogenous canopy areas were selected. The strong decrease in reflectance in the spectral domain of over 880 nm of the UHD 185 is due to a sensor problem and should be dismissed for further analysis.

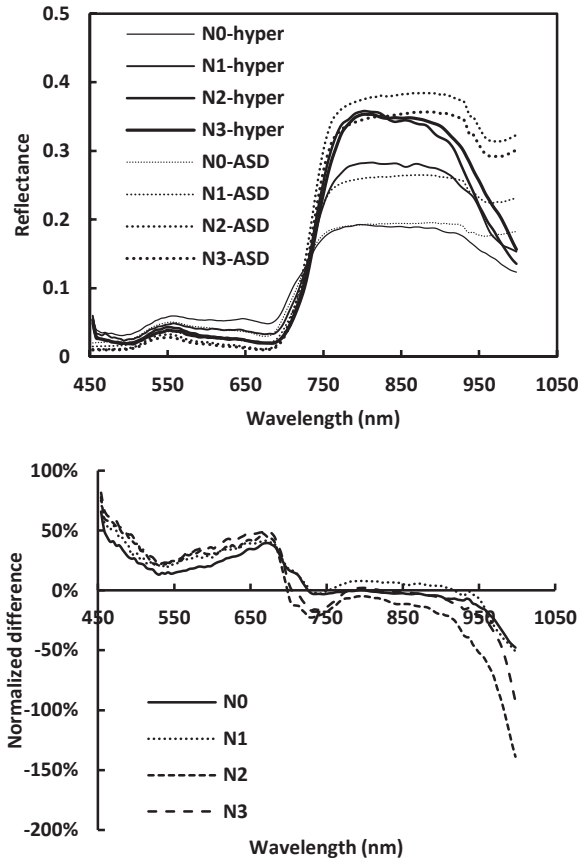

Fig. 2. Comparison of mean spectra derived from hyperspectral camera UHD 185 and spectra from hyperspectral field measurements with the ASD FieldSpec4 (upper); Spectral difference between mean spectra derived from hyperspectral camera UHD 185 and spectra from hyperspectral field measurements with the ASD FieldSpec4 (normalized difference = $(Ref_{image} - Ref_{ASD})/Ref_{image}$) (lower).

3.2. NDVI comparison between GS, ASD and hyperspectral camera

The derived spectral information from field measurements and from the UAV campaigns can be used to calculate well-established vegetation indices (VIs). As GS has only two central wavelength (774nm and 656nm), so the NDVI shown here is calculated with following formula: NDVI = (774 nm - 656 nm) / (774 nm + 656 nm) for unified comparison. The NDVI calculated from three sensors is shown in Fig.3.

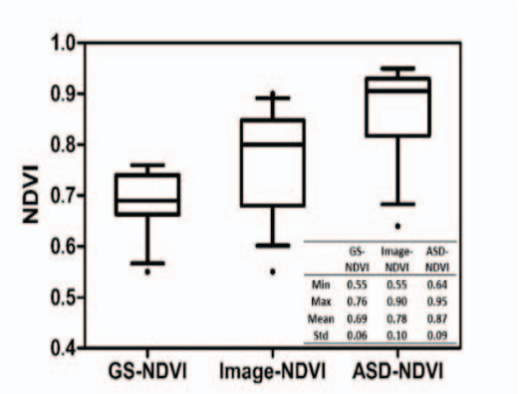

Fig. 3. Statistics of NDVI from different sensors (NDVI = (774 nm - 656 nm) / (774 nm + 656 nm)).

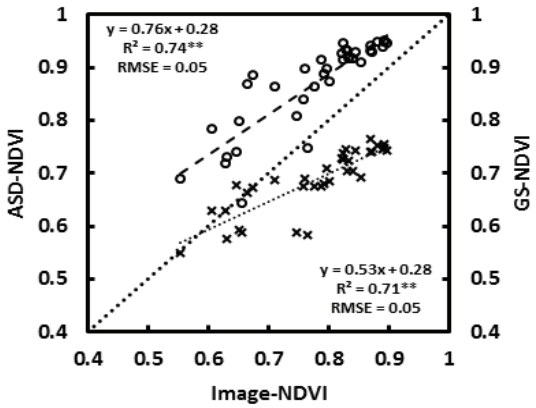

Fig. 4. Comparison of NDVI derived from hyperspectral camera UHD 185 and from the FieldSpec3 and GreenSeeker.

Compared with other two sensors, mean value of Image-NDVI is higher than GS-NDVI values, and lower than ASD-NDVI values. Image-NDVI has the widest range from 0.55 to 0.90, with a highest std of 0.10. The differences in Image-NDVI and ASD-NDVI, Image-NDVI and GS-NDVI values are all significant, with R^2 and RMSE of 0.74, 0.71, 0.05 and 0.05, respectively (Fig. 4).

3.3. Regression analysis results between spectral indices and rice leaf N concentration

Five VIs used for detecting nitrogen or chlorophyll were selected to estimate rice leaf nitrogen concentration. Table 2 shows the relationship of the VIs with the LNC derived from the hyperspectral camera. Compared with other indices, REP-Li yields best relationships with rice LNC, with R^2 and RMSE of 0.56 and 0.27, respectively (Table 2). MCARI/MTVI2 shows a relatively high coefficient of determination with LNC. Other VIs have a relative poor relationship with LNC, with R^2 below 0.4 and RMSE over 0.30 mg N g^{-1} d.m.

Table 2
Results of linear regression analysis between spectral indices and rice Leaf N concentration. The result (R^2) of best calibrated model were expressed in the table. ** indicates the statistical significance at 0.01.

Index	Regression equation	R^2	RMSE
Viopt	y = 1.38x - 2.59	0.31**	0.33
MCARI/MTVI2	y = -8.41x + 2.70	0.45**	0.30
R-M	y = 0.60x + 1.27	0.39**	0.31
REP-Li	y = 0.06x – 42.80	0.56**	0.27
NDVI	y = 2.32x + 0.10	0.28**	0.34

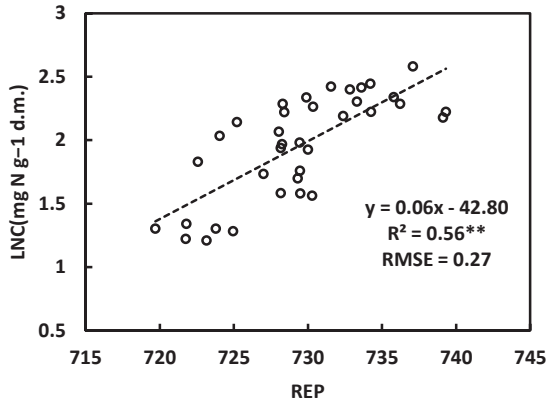

Fig. 5. Linear regression analysis result between leaf N concentration (mg N g^{-1} d.m.) and REP in rice; ** indicates the statistical significance at 0.01.

4. CONCLUSION

In this study, we assessed the data quality of one hyperspectral frame camera and evaluated the ability of this camera in rice nitrogen monitoring. The camera worked well and the flight campaign successfully delivered hyperspectral data. The result of spectral comparison between different sensors was satisfactory. Also, monitoring rice LNC using this hyperspectral camera was taken with a good performance. While this camera convinced with capturing the whole spectrum within one image with lower spatial resolution. More researches need to be done on the radiation correction. However, it is promising for the applications of Cubert's UHD 185 in precision agriculture.

5. REFERENCES

[1] J.M. Kim, H.J. Kim, K.H. Ryu, J.Y. Rhee, 2008. Fertilizer application performance of a variable-rate pneumatic granular applicator for rice production. Biosyst. Eng. 100 (4), 498–510.

[2] W. Li, G. Sun, Z. Niu, S. Gao, H.L. Qiao, 2014. Estimation of leaf biochemical content using a novel hyperspectral full-waveform LiDAR system. Remote Sens. Lett. 5 (8), 693–702.

[3] X.T. Ju, G.X. Xing, X.P. Chen, S.L. Zhang, et al. 2009. Reducing environmental risk by improving N management in intensive Chinese agricultural systems. Proceedings of the National Academy of Sciences of the United States of America, 106, 3041-3046.

[4] W. Feng, X. Yao, Y. Zhu, Y.C. Tian, W.X. Cao. 2008, Common Spectral Bands and Optimum Vegetation Indices for Monitoring Leaf Nitrogen Accumulation in Rice and Wheat. Europ. J. Agronomy, 28, 394–404.

[5] M. Quemada, J.L. Gabriel and P.Z. Tejada, 2014, Airborne Hyperspectral Images and Ground-Level Optical Sensors As Assessment Tools for Maize Nitrogen Fertilization, Remote Sens. 6, 2940-2962.

[6] J.S. Pearlman, P.S. Barry, C.C. Segal, J. Shepanski, D. Beiso, S.L. Carman, 2003. Hyperion, a space-based imaging spectrometer. IEEE Trans. Geosci. Remote Sens. 41, 1160-1173.

[7] M. Reyniers, D. J. J. Walvoort, & J. De Baardemaaker, (2006). A linear model to predict with a multi-spectral radiometer the amount of nitrogen in winter wheat. International Journal of Remote Sensing, 27, 4159−4179.

[8] J.U.H. Eitel, D.S. Long, P.E. Gessler, & A.M.S. Smith, (2007). Using in-situ measurements to evaluate the new RapidEye™ satellite series for prediction of wheat nitrogen status. International Journal of Remote Sensing, 28, 4183−4190.

[9] A.A. Gitelson, A. Viña, V. Ciganda, & D.C. Rundquist, (2005). Remote estimation of canopy chlorophyll content in crops. Geophysical Research Letter, 32, L08403.

[10] G. Guyot, F. Baret, & D.J. Major, (1988). High spectral resolution: Determination of spectral shifts between the red and the near infrared. International Archives of Photogrammetry and Remote Sensing, 11, 740−760.

[11] J.W. Rouse, R. H. Haas, J. A. Schell, D. W. Deering, and J. C. Harlan, (1974). Monitoring the vernal advancement of retrogradation (green wave effect) of natural vegetation. NASA/GSFC, Type III, Final Report, Greenbelt, MD, USA, pp. 1–371.